CHAPTER II
THEORETICAL BACKGROUND AND LITERATURE REVIEW

2.1 Background

Natural gas contains many contaminants, of which the most common undesirable impurity is water. Most natural gas contains water near saturation at the temperature and pressure of production. The dehydration of natural gas, which is a critical component of the natural gas conditioning process, is the removal of the water that is associated with natural gases in vapor form. Removal of water from the gas stream reduces the potential for corrosion, hydrate formation, and freezing in the pipeline. It stops sluggish flow conditions that may be caused by the condensation of water vapor in natural gas (Gandhidasan *et al.*, 2001). Hence, the dehydration of the natural gas is necessary.

2.1.1 Natural Gas Dehydration

One method to remove vapor water from natural gas is solid-desiccant dehydration, as illustrated in Figure 2.1. It is an adsorption process in which a solid adsorbent is used to adsorb molecules from the gas on the surface by surface forces. The operating temperature and pressure have an effect on the capacity of adsorption; that is, adsorption increases with a pressure increase and decreases with a temperature increase (Gandhidasan *et al.*, 2001). In the solid-desiccant dehydration unit, the wet gas enters the tower near the top, and flows downward through the solid desiccant on the adsorption cycle. The equilibrium zone, adsorbent saturated with vapor water, propagates from the top layer and moves down to the next layer. The equilibrium zone continually increases along the reactor until all of the adsorbents are saturated with water.
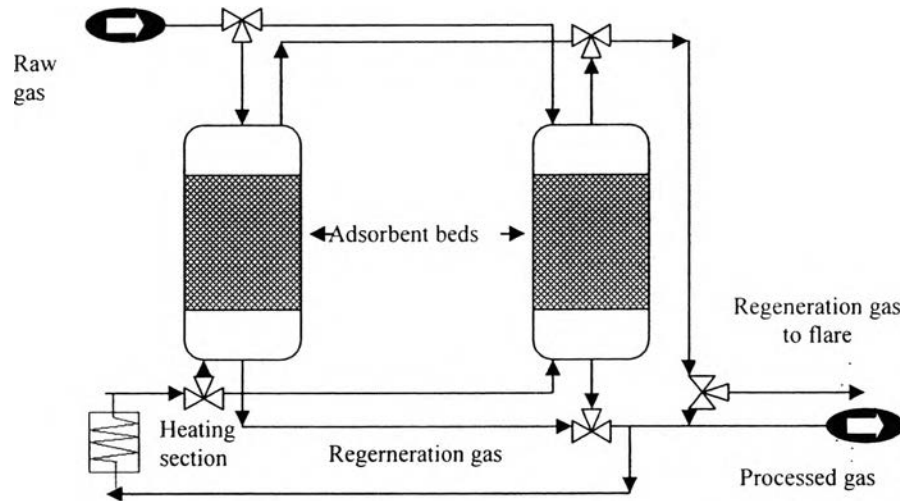
Figure 2.1 Dehydration by adsorption (Rojey *et al.*, 1997).

2.1.2 <u>Adsorbent Materials</u>

The adsorbent materials which can be selected for use in the dehydration system should have the following characteristics: large surface area for high capacity, high mass transfer rate, and easy and economical regeneration ability, good activity retention with time, and high mechanical strength to resist crushing and dust formation, and so forth. Examples of materials with the above mentioned characteristics are activated alumina, molecular sieve, and silica gel, etc.

2.1.2.1 Activated Alumina

Activated alumina is produced from bauxite ($Al_2O_3 \cdot 3H_2O$). It has high porosity resulting in high surface area. The surface of activated alumina is strongly polar, so it can adsorb polar molecules such as water. Activated alumina is usually used for drying warm gas because it has high capacity at elevated temperatures (Ruthven, 1984).

2.1.2.2 Silica Gel

Silica gel is one form of silica SiO_2 that has a high porosity. It can be produced from the sodium silicate solution or the hydrolysis of soluble alkali metal silicates with acid. The surface of silica gel has a polar state on which

molecules such as water, alcohols, phenols, and amines and saturated hydrocarbons can be adsorbed in preference to nonpolar molecules (Ruthven, 1984).

2.1.2.3 Molecular Sieves

Molecular sieves are alkali metal crystalline aluminosilicates. This crystal consists of pores that have a certain size. The diameter of porosity changes with the type of charge-balancing cations such as 4A molecular sieves composed of Na_2O_3, Al_2O_3, and SiO_2. Molecular sieves have their polar property on the inner surface of the crystal cavities, which are attracted to polar molecules in preference to non-polar molecules (Campbell, 1984).

2.1.3 Deactivation

The adsorption capacity of an adsorbent decreases with time of operation, possibly because of either pore mouth closure, window blocking, coking, or hydrothermal decrystallization. These phenomena can occur from hydrothermal streaming or in presence of residue hydrocarbons (Khan and Loughlin, 2003). Adsorption capacity can be explained in terms of activity. For separable kinetic, the activity of catalyst, a(t), is defined as the ratio of the rate of reaction on a catalyst that has been used for a time, t, to the rate of reaction on a fresh catalyst ($t=0$) (Fogler, 2006):

$$a(t) = \frac{-r_A'(t)}{-r_A'(t = 0)}$$
(2.1)

And the rate of catalyst decay can be expressed as:

$$r_d = -\frac{da}{dt}$$
(2.2)

2.1.4 Monolayer and Multilayer Adsorption

The isotherms for physical adsorption have been divided into five classes by Brunauer et al., as illustrated in Figure 2.2. Type I and type V show that the pore size of the adsorbent is not much higher than the adsorbate molecule, so adsorbents have a limitation to adsorb the adsorbate molecules. An adsorbent with a wide range of pore sizes can adsorp the adsorbate molecule on the surface from

monolayer to multilayer adsorption and then to capillary condensation, as shown in Types II and III. An isotherm of Type IV implies that the adsorption occurs on two surface layers; either on a plane surface or on the wall of a pore highly wider than the adsorbate molecule (Ruthven, 1984).
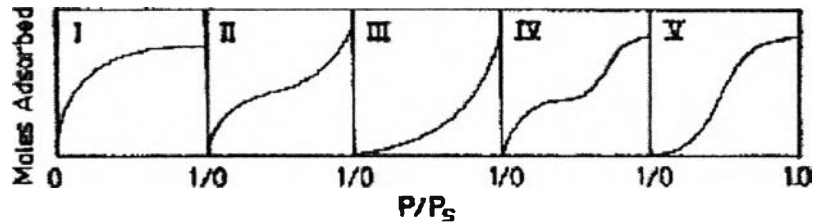

Figure 2.2 Adsorption isotherm classifications according to Brunauer *et al.* (1940).

Various equations of adsorption isotherms have been developed to explain the adsorption on the adsorbent. In order to obtain the proper equation for each case study, the following equations were introduced.

Equations reducible to Langmuir isotherm (Toth, 2002):

$$\frac{q}{q_s} = \left(\frac{(Kp)^m}{1 + (Kp)^m} \right)^{f/m} \qquad (2.3)$$

The various adsorption isotherms can be shown by different conditions of the parameters in above equation as follows:

f = m = 1; The Langmuir relation isotherm.

f = m ≠ 1; The Langmuir- Freundlich isotherm (LF).

m = 1 and f ≠ 1; The generalize Freundlich isotherm (GF).

m ≠ 1 and f = 1; The Toth isotherm (I).

Isotherms generated by the exponential isotherm equation (Toth, 2002):

$$\frac{q}{q_s} = \exp\left(-\sum_{j=1}^{\cdot} E_j\left[k_B T \ln\left(\frac{p_a}{p}\right)\right]\right)^j \tag{2.4}$$

This equation can be reduced to other equations by the following case:

$B_1 > 0$ and $B_j = 0$ for $j \geq 2$; The classical Freundlich isotherm (F).

$B_2 > 0$ and $B_j = 0$ for $j \neq 2$; The Dubinin-Radushkevich isotherm (DR).

$B_j > 0$ and $B_i = 0$ for $j \neq i$; The Dubinin-Astakhov isotherm (DV).

B_1 , $B_2 > 0$ and $B_j = 0$ for $j>2$; The Freundlich-Dubinin-Radushkevich isotherm (FRD).

The UNILAN isotherm equation (Rodrigues et al., 1989):

$$\frac{q}{q_s} = \frac{1}{2s}\ln\left[\frac{1+Cpe^{+s}}{1+Cpe^{-s}}\right] \tag{2.5}$$

The TALAN isotherm equation (Rodrigues et al., 1989):

$$\frac{q}{q_s} = \frac{Kp}{1+Kp} + \frac{\sigma^2 Kp(1-Kp)}{2(1+Kp)^3} \tag{2.6}$$

The Ruthven and Longhlin isotherm equation (Rodrigues et al., 1989):

$$\frac{q}{q_s} = \frac{Kp + \sum_i\left[\frac{(Kp)^i(1-ib)^i}{(i-1)!}\right]}{1+Kp+\sum_i\left[\frac{(Kp)^i(1-ib)^i}{i!}\right]} \tag{2.7}$$

The BILAN isotherm equation (Rodrigues *et al.*, 1989):

$$\frac{q}{q_s} = \sum_{i=0}^{n} \theta_i(p,\varepsilon_i) p_i(\varepsilon_i) \qquad (2.8)$$

where

$$\theta_i = \frac{C_i p}{1 + C_i p}$$

$$C_i = C_o e^{\varepsilon_i / kT}$$

$$\varepsilon_i = \bar{\varepsilon} + \frac{i - np}{\sqrt{np(1 - p)}} \sigma$$

$$p_i(\varepsilon_i) = \binom{n}{i} p^i (1 - p)^{n-i}$$

$$\gamma = \frac{1 - 2p}{\sqrt{np(1 - p)}}$$

The Henry isotherm equation (Ruthven, 1984):

$$\frac{q}{q_s} = bp \qquad (2.9)$$

The BET isotherm equation (Ruthven, 1984):

$$\frac{q}{q_m} = \frac{b(p/p_s)}{(1 - p/p_s)(1 - p/p_s + bp/p_s)} \qquad (2.10)$$

For the deactivated adsorbent, the adsorption capacity will decrease with the deactivation of the adsorbent resulting in a change in the adsorption isotherms. The slope of the adsorption isotherm will decrease. becoming more flat with the degree of deactivation (Rodrigues *et al.*, 1989). as illustrated in Figure 2.3.
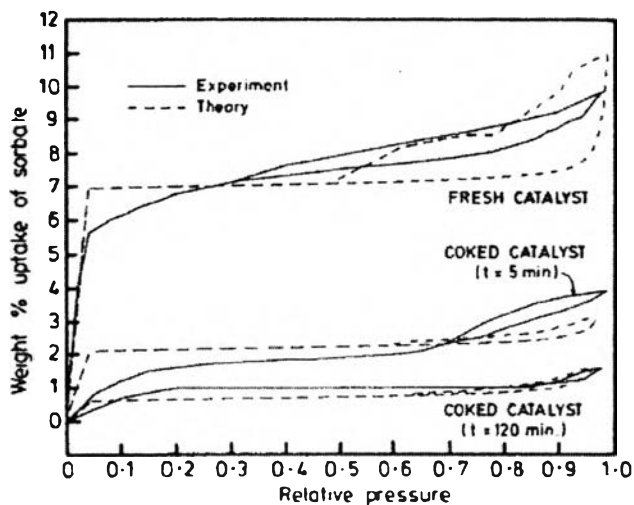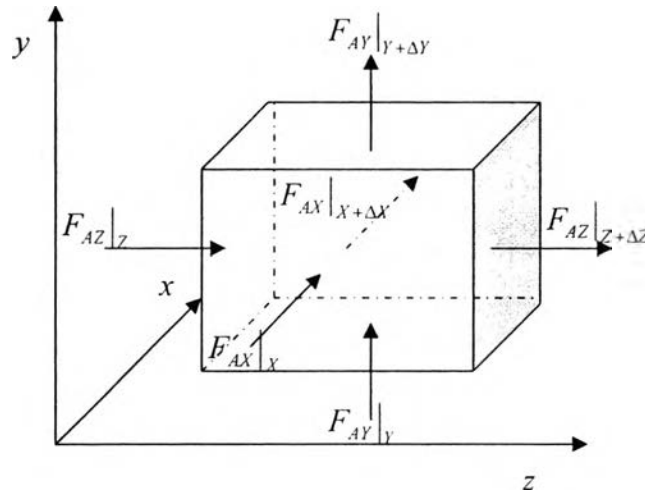
Figure 2.3 The adsorption isotherm change with age of deactivation (Rodrigues *et al.*, 1989).

2.1.5 Regeneration

In order to recover a saturated adsorbent, the regeneration process is introduced into the dehydration of the natural gas system. The dry gas from adsorption step is utilized for the regeneration process. This gas is heated by a heat exchanger using steam or hot oil from about 200 to 325°C. At the beginning, the tower and the desiccant are heated to about 120°C by the hot gas. At this temperature, water is boiled or vaporized. and the bed continues to be heated, but more slowly because water is being removed from the desiccant. The hot gas still continually heats up the desiccant after all water has been removed in order to eliminate any heavier hydrocarbons and contaminants. After the regeneration process is finished, the bed is then cooled before it is changed to the adsorption mode (Gandhidasan *et al.*, 2001).

2.1.6 Mathematical Model

If a small volume of any system ($\Delta V = \Delta x \Delta y \Delta z$) is considered, the mole balance can be employed to explain the variation of molar fluxes of a species A in three dimensions (Fogler. 2006).

$$\sum_i \begin{bmatrix} Molar \\ flow\ rate \\ in \end{bmatrix}_i - \sum_i \begin{bmatrix} Molar \\ flow\ rate \\ out \end{bmatrix}_{i+\Delta i} + \begin{bmatrix} Rate\ of \\ generation \end{bmatrix} = \begin{bmatrix} Rate\ of \\ accumulation \end{bmatrix}$$

So, the mole balance is:

$$\sum_i F_{Ai}\big|_i - \sum_i F_{Ai}\big|_{i+\Delta i} + r_A \Delta x \Delta y \Delta z = \Delta x \Delta y \Delta z \frac{\partial c_A}{\partial t} \qquad (2.11)$$

where

i refers to each component (x, y, z)

$F_{Az} = W_{AZ}\Delta x \Delta y$

$F_{Ay} = W_{Ay}\Delta x \Delta z$

$F_{Ax} = W_{Ax}\Delta z \Delta y$

The molar flux balance in rectangular coordinates can be determined by dividing all of Equation 2.11 by $\Delta x \Delta y \Delta z$ and taking their limit to zero.

$$-\frac{\partial W_{Ax}}{\partial x} - \frac{\partial W_{Ay}}{\partial y} - \frac{\partial W_{Az}}{\partial z} + r_A = \frac{\partial c_A}{\partial t} \qquad (2.12)$$

By the assumption of no variation in r and θ direction in cylindrical coordinates, the mass balance is:

$$-\frac{\partial W_{Az}}{\partial z} + r_A = \frac{\partial c_A}{\partial t} \tag{2.13}$$

The molar flux of A in z direction, W_{Az} consists of two parts which are the molecular diffusion flux relative to bulk motion of the fluid produced by a concentration gradient, and the flux resulting from the bulk motion of the fluid (Fogler, 2006):

$$W_{Az} = -D_L \frac{dc_A}{dz} + c_A v_z \tag{2.14}$$

In this work r_A is the rate adsorbate concentration averaged on adsorbent:

$$r_A = \left(\frac{1-\varepsilon}{\varepsilon}\right)\frac{\partial \overline{q}}{\partial t} \tag{2.15}$$

By applying the influence of deactivation as explained in the previous part, a (t) = r_A (t)/ r_A (t=0), into this rate, the rate at any time is:

$$r_A = a(t)\left(\frac{1-\varepsilon}{\varepsilon}\right)\frac{\partial \overline{q}}{\partial t} \tag{2.16}$$

After substituting r_A and W_{Az} into Equation (2.13), the equation can be re-written as:

$$-D_L \frac{\partial^2 c_A}{\partial z^2} + \frac{\partial}{\partial z}(vc_A) + \frac{\partial c_A}{\partial t} + a(t)\left(\frac{1-\varepsilon}{\varepsilon}\right)\frac{\partial \overline{q}}{\partial t} = 0 \tag{2.17}$$

where

D_L = axial dispersion coefficient

v = interstitial velocity

ε = voidage of adsorbent bed

$\overline{q}$ = adsorbate concentration averaged over crystal and pellet

t = time

z = distance measured from column inlet

c_A = adsorbate concentration in fluid phase

The last term of the above equation ($\frac{\partial \bar{q}}{\partial t}$) can be expressed in the linear rate

expression (Ruthven, 1984):

$$\frac{\partial \bar{q}}{\partial t} = k(q^* - \bar{q}) \qquad (2.18)$$

where k and q^* is the overall mass transfer coefficient and the equilibrium adsorbed

phase concentration, respectively.

2.2 Literature Survey

The experiment and mathematical modeling of breakthrough time for the dehydration of a natural gas system were applied by Chaikasetpaiboon (2003), in which the adsorber consisted of two types of adsorbents, which are silica gel, 4A molecular sieve of size 1/8" and molecular sieve of size 1/16". The mathematical model was presented by the axial dispersion plug flow model based on mass balance as the following:

$$-D_L \frac{\partial^2 c}{\partial z^2} + \frac{\partial}{\partial z}(\upsilon c) + \frac{\partial c}{\partial t} + \left(\frac{1-\varepsilon}{\varepsilon}\right)\frac{\partial \bar{q}}{\partial t} = 0 \qquad (2.19)$$

The equilibrium adsorption isotherms of this work come from passing fluid through an adsorber which consists of three adsorbents. They can be separated into two regions: one is the Longmuir model, which explains at a humidity level less than 52% RH, another one is the Linear model, which accords at above 52% RH. The overall mass transfer coefficient was suggested to be about 1.0×10^{-4}, which was acceptable for all experiments. In order to solve the natural gas concentration. c(z,t), in fluid phase. the method of lines with central finite definition difference and Runge-Kutta 4th was utilized in this work. The breakthrough time from this model was shorter than from the experiments by about 27%.

In the year 2004, Uttamaroop followed the work of Chaikasetpaiboon to develop the mathematical model. In this work, the equilibrium adsorption isotherm was constructed for each adsorbent instead of for all of the adsorbents in adsorber, as in Chaikasetpaiboon's work. In Uttamaroop's work, the sensitive parameters were analyzed, and it was found that the interstitial velocity (v) and bed voidage (ε) were sensitive with a changing of the breakthrough curve more than the axial dispersion coefficient (D_L). So, it was assumed that the interstitial velocity of the feed gas was not constant along the reactor. Afterwards, it was found that this assumption did not have more of an effect on the change of the breakthrough curve when compared with the interstitial velocity constant. Moreover, the breakthrough time was found to decrease with increasing relative humidity and velocity of inlet gas. In order to best fit between the experimental and theoretical breakthrough curve, an overall mass transfer coefficient of about $8.5 \times 10^{-5} s^{-1}$ was offered. In this work, the breakthrough time of the experiments was different from the mathematical model about 3% to 5%.

Khaikham (2007) studied the mathematical model of breakthrough curve of the multi-layer gas adsorber containing two types of adsorbents; activated alumina and molecular sieve zeolite type 4A. The change of physical property in both fresh and deactivated adsorbents was studied. Hydrothermal steaming in the regeneration step is cause of deactivation of such adsorbents. Experiments showed that hydrothermal steaming decreased in the specific surface area of activated alumina and in average crystal size of the molecular sieve zeolite. The percentage of deactivation for activated alumina and molecular sieve zeolite type 4A was achived to about 90% and 15%, respectively, and the equilibrium adsorption isotherm for each status of the adsorbent was taken into the axial dispersion plug flow model, as in Uttamaroop's work, in order to find the breakthrough time of this process. It was shown that the breakthrough time of the deactivated bed was shorter than the fresh one, and the predicted breakthrough time from the model is in accord with the experiments.

Zhang and Cheng (2000) found a mathematical model to describe the removal of cyanogen chloride (CNCl) from a gas stream passing through a fixed bed adsorptive reactor in which activated carbon impregnated with copper, chromium, and silver was used as an adsorbent. The catalytic hydrolysis reaction of cyanogen

chloride, because of the presence of moisture, as well as the oxidation–reductive reaction of activated carbon impregnated with copper, chromium, and silver, occur in this process and affect the deactivation of the catalyst. The continuity equation of fixed bed was assumed to be a for first-order deactivation and was referred to by the following:

$$\frac{\partial c}{\partial t} + v\frac{\partial}{\partial x}c + \left(\frac{1-\varepsilon}{\varepsilon}\right)\frac{\partial q}{\partial t} + R = 0; \quad R = KCe^{-K_d t} \tag{2.20}$$

The experiments show that the mathematical model by deactivation rate constants (K_d) of CNCl in different carbon beds obtained from the linear regression that depend on the experimental conditions agree with the practical deactivation characteristics of the carbons.

Kopac and Kocabas (2002) investigated the sulfur dioxide adsorption characteristics on silica gel, in the form of 0.1–0.3 mm size granules packed in stainless steel columns of 0.1 m length and 0.0095 m diameter to obtain the adsorption isotherms of sulfur dioxide on silica gel. The experiments were operated at 473 K constant temperature with different sulfur dioxide inlet concentrations in the range of 430–3400 ppm and constant sulfur dioxide inlet concentration of 1610 ppm for temperatures of 373 and 473 K, in addition to 1500 ppm. at 323 K. Freundlich adsorption isotherms gave the best fit for this work. Moreover, they applied the deactivation model proposed by Suyadal et al. (2000) to analyze the breakthrough curve by comparing the experimental, and model results in the same condition for investigating the adsorption isotherms. The experimental data agree with the deactivation model predictions, implying a significant deactivation of the adsorbent with time with respect to probable changes in pore structure, in the active surface area, and active site distribution of the adsorbent.

Kopac and Kocabas (2004) analyzed the breakthrough data for sulfur dioxide on silica gel by comparing the results of the deactivation models proposed by Orbey et al. (2001) and Yasyerli et al. (2001). The deactivation model of Orbey et al. (1982) for the breakthrough of solid-gas taking place in a packed bed reactor can be expressed as follows:

$$\frac{c}{c_0} = \left[e^{Nv} \frac{\sinh[\phi_0 \exp(-N\theta)]}{\sinh[\phi_0 \exp N(v - \theta)]} \right]^{\frac{\delta}{N}}$$

(2.21)

And a model for predicting the breakthrough curve was proposed by Yasyerli *et al.* as follows:

$$\frac{c}{c_0} = \exp\left[\frac{\left[1 - \exp\left(\frac{k_0 W}{Q} (1 - \exp(-k_d t)) \right) \right]}{[1 - \exp(-k_d t)]} \exp(-k_d t) \right]$$

(2.22)

The Orbey *et al.* (1982) model included intrapellet diffusion resistance, but in the Yasyerli *et al.* (2001) model, internal diffusion resistance was neglected. However, concentration dependence was considered in this model. The parameters of both models for sulfur dioxide adsorption were shown at 323, 373, and 473 K and the inlet concentration at these temperatures are 0.2264, 0.2104, and 0.1659 mol/m^3, respectively. Moreover, the parameters of both models were investigated at 473 K for sulfur dioxide inlet concentration in the range of 0.0443-0.3504 mol/m^3 as well. Analysis of both deactivation models shows that these models can be applied to investigate the adsorption of sulfur dioxide on silica gel, and the parameter of the Orbey model was more different than the parameter of the Yasyerli model when vary conditions, so the latter model is the best one for analyzing the breakthrough curve of sulfur dioxide adsorption.

In recent work, the characterizations of deactivated adsorbents were studied. Also, the adsorption isotherms of each adsorbent were performed at various percentages of deactivation, and theoretical breakthrough time was investigated for all possible bed compositions. Especially, these were studied at low degree of deactivation. Therefore, the main purpose of this work was to describe the dynamic behavior of water vapor removed from natural gas using a multilayer adsorber packed with fresh and deactivated adsorbents. Additionally, the physical properties and adsorption isotherms of deactivated adsorbents at high percentages of deactivation were determined. Moreover the change in interstitial velocity due to

pressure drop along the adsorber was applied in the breakthrough time model, and the parameters in the breakthrough time equation changing with the percentage of deactivation were investigated to modify the breakthrough time model in accordance with deactivation.